Melissa M. Scott-Pandorf[1]
e-mail: mmscottp@gmail.com

Daniel P. O'Connor

Charles S. Layne

Laboratory of Integrated Physiology, Health, and Human Performance,
University of Houston,
Houston, TX 77204

Krešimir Josić
Department of Mathematics,
University of Houston,
Houston, TX 77204

Max J. Kurz[1]
Laboratory of Integrated Physiology, Health, and Human Performance,
University of Houston,
Houston, TX 77204;
Laboratory of Motion Analysis,
Munroe-Meyer Institute,
University of Nebraska Medical Center,
Omaha, NE 68198-5450
e-mail: mkurz@unmc.edu

Walking in Simulated Martian Gravity: Influence of the Portable Life Support System's Design on Dynamic Stability

With human exploration of the moon and Mars on the horizon, research considerations for space suit redesign have surfaced. The portable life support system (PLSS) used in conjunction with the space suit during the Apollo missions may have influenced the dynamic balance of the gait pattern. This investigation explored potential issues with the PLSS design that may arise during the Mars exploration. A better understanding of how the location of the PLSS load influences the dynamic stability of the gait pattern may provide insight, such that space missions may have more productive missions with a smaller risk of injury and damaging equipment while falling. We explored the influence the PLSS load position had on the dynamic stability of the walking pattern. While walking, participants wore a device built to simulate possible PLSS load configurations. Floquet and Lyapunov analysis techniques were used to quantify the dynamic stability of the gait pattern. The dynamic stability of the gait pattern was influenced by the position of load. PLSS loads that are placed high and forward on the torso resulted in less dynamically stable walking patterns than loads placed evenly and low on the torso. Furthermore, the kinematic results demonstrated that all joints of the lower extremity may be important for adjusting to different load placements and maintaining dynamic stability. Space scientists and engineers may want to consider PLSS designs that distribute loads evenly and low, and space suit designs that will not limit the sagittal plane range of motion at the lower extremity joints. [DOI: 10.1115/1.3148465]

Keywords: Floquet, gravity, load, walk, gait

1 Introduction

Due to recent aspirations to extend space exploration to Mars, NASA has a revitalized interest in reduced gravity locomotion for designing the next generation of space suits. A new suit, to be worn during extravehicular (EVA) tasks, must provide life-sustaining supplies without inhibiting the astronauts' ability to perform tasks on the surface of Mars. Review of the video archives from the Apollo missions on the Moon revealed an issue of repeated instances of the astronaut losing balance and falling. Several factors, including uneven terrain, suit construction, reduced gravity, and the portable life support system (PLSS) could have potentially influenced the astronaut's balance. Although all factors play a role in the astronauts' stability, redesign of the PLSS is possible for improved walking stability. By altering the construction of the PLSS to have a different load distribution, there may be improvements in the dynamic stability of the astronaut's gait while traversing the surface of Mars.

Some studies have explored load placement while walking in Earth's gravity. In general, equally distributed loads on the front and back, and loads closer to the torso were found to be superior to other carrying modes and load placements [1–5]. Their findings indicated, in most cases, that loads distributed evenly on the front and back decreased forward lean, increased low back comfort, and decreased energy expenditure compared with a load placed only on the back [1,3–5]. In a comparison of a backpack and front-backpack, the front-backpack displayed walking kinetics and kinematics that more closely resembled walking without load [2]. However, in either load distribution case, carrying loads resulted in decreased single support time, increased double support time, increased step width, increased ground reaction forces, and increased knee flexion [2]. Interestingly, many of these kinematic changes have been recognized as potential mechanisms for improving the stability of the gait pattern [6,7]. However, no study has directly investigated the dynamic stability of the gait pattern while carrying additional weight in various load placements. Intuitively, loads placed closer to the torso, evenly distributed, and lower on the body would be less likely to impact the dynamic stability of locomotive system. In fact, as early as 1869, it was recommended that military officers carry loads lower and closer to the body in order to maintain the greatest stability while walking [8]. To our knowledge, no research has ever tested this idea directly. Furthermore, reduced gravity environments could pose their own challenge on the locomotive system. The influence of load location on the dynamic stability of the gait pattern in a Martian environment is unknown. This information may be essential for the development of the next generation of PLSS and the prevention of walking instabilities during future Mars EVA missions.

A single Mars mission will be approximately a 900 day commitment and is likely to include four times as many EVAs as the entire history of the space exploration program [9]. Based on this notion, the ergonomic properties of the PLSS are important for improving mobility and dynamic balance while performing EVAs. Review of the Apollo video archives revealed astronauts tumbling forward repeatedly. These falls could result in reduced productivity, injury to equipment or the space suit, and injury to the astronaut. Although, the gravity on Mars is 3/8 of Earth gravity it

[1]Corresponding author.

Contributed by the Bioengineering Division of ASME for publication in the JOURNAL OF BIOMECHANICAL ENGINEERING. Manuscript received August 22, 2008; final manuscript received May 1, 2009; published online August 5, 2009. Review conducted by Richard Neptune. Paper presented at the 2008 North American Congress of Biomechanics.

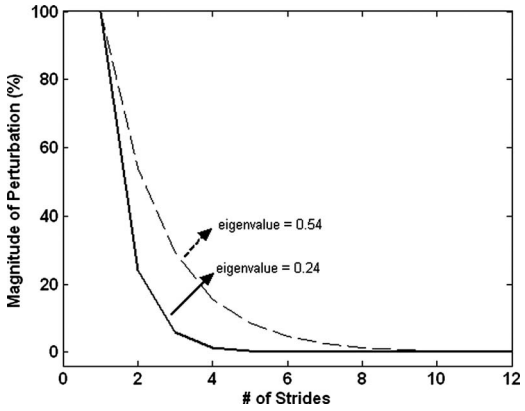

Fig. 1 Eigenvalues signify the rate of recovery from a perturbation over multiple strides. The smaller eigenvalue (0.24) takes approximately five strides to recover while the larger eigenvalue (0.54) takes approximately ten strides to recover.

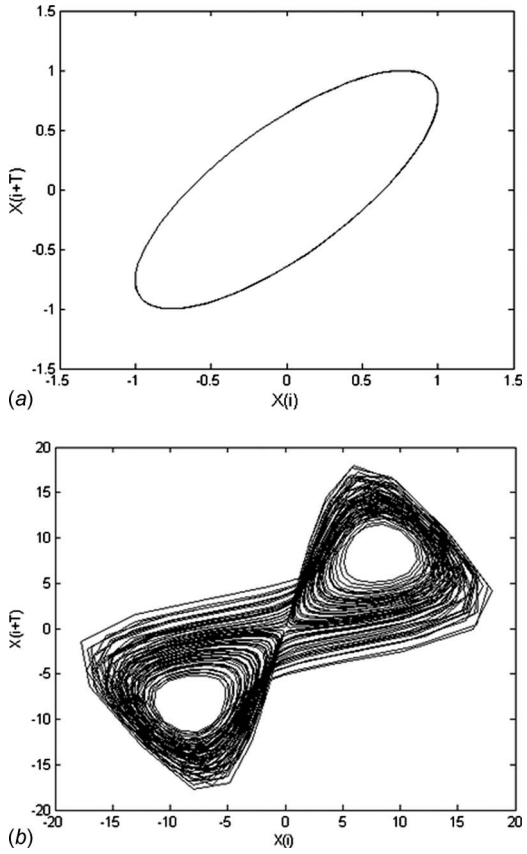

Fig. 2 (*a*) No divergence is present in the attractor for a harmonic oscillator and the maximum LyE is 0. (*b*) The *x* component of the Lorenz attractor contains more divergence and has a maximum LyE of 1.5.

cannot be discounted. Falling in the suit onto a sharp object among the Martian terrain could certainly puncture a suit or falling with important geographical equipment could break the device. Apollo lunar journals have noted various equipment breaking as a result of tripping or clumsiness on the Moon's surface, which is an environment of just 1/6 Earth's gravity. Additionally, the consequence of visiting Mars includes a considerable delay in communication with Earth requiring the astronauts on these missions to be largely autonomous. Therefore, there is a need to evaluate simulated Martian gravity locomotion stability based on various PLSS designs.

Attempts to quantify changes in gait stability on Earth have ranged from observing differences in the joint angular displacements, variations in the stepping pattern [10–13], and responses to external perturbations that induce a slip or trip during gait [14–17]. Resilience of the locomotive system to external perturbations is often considered the gold standard for quantifying stability. A dynamically stable locomotive system is capable of resisting larger perturbations that may cause a fall, and will return back to the steady state gait pattern at a faster rate after a perturbation is encountered. However, gait perturbation analysis methods do have limitations since the participant often switches to a guarded gait after the first perturbation trial [15]. This may limit the range of perturbations that can be used when exploring the limits of stability. Alternative metrics that provide similar information as the perturbation analysis are necessary to determine the dynamic stability of the gait pattern while walking with the PLSS in a reduced gravity environment.

Stability of a dynamical system can mathematically be defined based on how the state variables (i.e., angular displacements and velocities) respond to external or internal perturbations (e.g., neuromechanical errors) [18,19]. Based on the notion that the dynamics of the system are strictly periodic, Floquet analysis (FA) quantifies the ability of the system to return back to a fixed point in the cycle (e.g., knee angle at midswing) after encountering a perturbation. The rate of convergence or divergence from the fixed point is based on the eigenvalues of the Jacobian, which defines the rate of change in the cycle-to-cycle dynamics. An eigenvalue closer to zero indicates that the locomotive system will rapidly recover from a perturbation and return back to the fixed point in the limit cycle, while eigenvalues closer to one indicate a slower recovery back to the fixed point [20]. For example, an eigenvalue of 0.24 indicates that 24% of the perturbation remains after a gait cycle [18], and that this perturbation will be asymptotically reduced over the next consecutive gait cycles (e.g., 5.76% after two gait cycles, 1.38% after three gait cycles, etc.; Fig. 1). A system with a larger eigenvalue is considered less stable because it takes longer for the locomotive system to return back to the steady-state gait pattern, and has a higher probability of falling if an additional perturbation is encountered during the recovery period [18,20,21]. The use of the eigenvalues to evaluate the dynamic stability of the gait pattern has been well supported by experiments with walking robots and has been successfully used to distinguish between fallers and nonfallers in the aging population [22]. Potentially, FA may also provide insight on the dynamic stability of the locomotive pattern while walking with a PLSS in a simulated Martian environment.

FA evaluates the ability to return back to a fixed point in the gait cycle because it assumes that the oscillatory dynamics of the lower extremity are strictly periodic. However, human locomotion is not strictly periodic and has subtle variations in the cycle-to-cycle dynamics. The stroboscopic approach of FA ignores the local instabilities that are present in the gait cycle [23]. In contrast, the Lyapunov exponents (LyEs) are well suited for evaluating the local instabilities present in aperiodic systems because they evaluate the rate at which nearby trajectories in the state space diverge over time [23,24]. The larger the average value of the largest LyE computed for a finite times along the attractor, the greater the amount of dynamic instability present in the attractor dynamics [23]. For example, the attractor for a harmonic oscillator that has no local divergence has a largest LyE of zero [25]. Alternatively, evaluating the x coordinate of the Lorenz attractor ($\sigma=16$, $R=45.92$, and $b=4$) has a high amount of average local divergence, and the largest LyE is estimated to be 1.5 (Fig. 2) [24]. Previous investigations have indicated that the average local divergence rates along the attractor flow are an indicator of the system's resistance to small local perturbations that arise from the neuromechanical couplings of the locomotive system [7,26,27]. Furthermore, recent computer simulations from walking models indicate

that if these local instabilities grow large enough they may result in a fall [28]. Evaluating the average local instabilities present in the locomotive attractor may provide a complementary approach for further quantifying the dynamic stability of the gait pattern while walking with a PLSS in a simulated Martian environment.

Floquet and Lyapunov analysis methods offer new complementary means for classifying the dynamic stability of the gait pattern. The purpose of this investigation was to explore the dynamic stability of the lower extremity joint kinematics in a simulated Martian gravity while wearing a rig that simulates the possible load placements of the PLSS that astronauts may wear. This scientific information will advance our understanding of how load placement influences the dynamic stability of the gait pattern and will guide the construction of the next generation of PLSS that will be used for EVAs on Mars.

2 Methods

2.1 Participants. Six females and four males (69.7 ± 11.7 kg, 170.2 ± 5.0 cm, and 24.6 ± 6.5 yr) participated in the experiment. An a priori power analysis using pilot data exhibited 96% power would be attained with nine or more participants ($f = 0.38-0.44$, alpha$=0.01$, 1$-$beta$=0.95$). Alpha was set to 0.01 to account for multiple comparisons that would be made if an analysis of variance (ANOVA) was found to be significant. Inclusion criteria required participants be between the ages of 18 and 45 and regularly physically active (i.e., exercise three times per week for at least 30 min). Participants were excluded if they were not able to pass the physical activity readiness questionnaire (PAR-Q), have a previous history of musculoskeletal injury or neurological injury that may influence locomotion, and weigh more than 84 kg. The inclusion/exclusion criteria were selected in order to secure the safety of the participants in the study. Although the participants may have similar fitness levels to the astronaut populations based on inclusion/exclusion criteria, the recruitment of participants was based on a volunteer basis among the university staff and students. Therefore, the participants in this experiment were not matched to the astronaut population.

2.2 Apparatus. To simulate Martian gravity (3/8 Earth gravity) a custom bodyweight suspension system (BWSS) was built. The suspension system frame was constructed with Telespar®, and an overhead trolley system (DeMag Cranes and Components, Cleveland, OH) was attached to the frame. The trolley allowed the participants in the system to move in the anterior/posterior direction while walking on a treadmill (Biodex Medical Systems Inc., RTM 4000, Shirley, NY). The suspension part of the system was composed of a series of climbing rope (REI Inc., Sumner, WA) and surgical tubing (VWR International, West Chester, PA). The climbing rope was fed into a winch, and this winch was cranked to adjust the offloading force being applied to participants by stretching the surgical tubing. The force was recorded using a strain gauge force transducer (i.e., load cell; Omegadyne Inc., Sunbury, OH) that was in series with the overhead attachment of the participant. In this investigation, the force transducer output indicated our offloading goals fluctuated by 7%. The participants were attached to the suspension system with a hip harness that is typically used for acrobatics (Barry Cordage, Ltd., Montreal, Quebec).

We used a custom PLSS rig that simulated the possible load placements for the PLSS (Fig. 3). The PLSS rig was constructed of 8020 (8020® Inc., Columbia City, IN) and allowed for parts of the system to be reconfigured in the possible load placement configurations (Fig. 4). The PLSS rig attached to the participants using basic shoulder straps and a waist belt used for climbing packs (Fig. 3). The configurations of the rig include normal, low, high, forward, and aft. Normal referred to a load position, which was evenly distributed at the sides of the torso and maintained the load near the body's natural center of gravity (CG). Low, high, forward, and aft referred to alternate locations of the load. Weights were applied to an extrusion arm on the rig to create the specific load placement conditions (Fig. 3). Without the weights the PLSS rig's mass was 15.5 kg, and with the additional weights the total mass was 20 kg.

Fig. 3 Demonstration of how the PLSS rig fits on a participant. Backpack straps and a waist belt secure the rig onto the participant. Weights were applied to the back extrusions of the PLSS rig to create the aft condition here. Retroreflective markers were placed on the participant's heel, metatarsal-phalange joint, lateral malleolous, lateral epicondyle, greater trochanter, and acromion-clavicle joint.

The added load on the extrusion arms were set to 4.5 kg. With a load of 4.5 kg the pilot study participants were able to walk with the PLSS rig on and could select a speed, in which all conditions could be performed.

2.3 Protocol. Participants visited the Laboratory of Integrated Physiology on two separate days. On the first day the participants were informed of the study purpose, protocol, risks, and benefits according to the Committee for Protection of Human Subjects and filled out a PAR-Q [29]. Participants went through the study protocol without any actual data being collected. The purpose for the first visit to the laboratory was for the participants to acclimate to the novel task of walking in simulated Martian gravity with the PLSS rig on.

On this first day, a self-selected pace (0.88 ± 0.05 m/s) was determined by the participants while offloaded to 3/8 gravity without the PLSS rig on. During pilot testing, it was revealed that the participants' self-selected pace while walking without the PLSS rig was too fast to stay on the treadmill belt once the participants were wearing the PLSS rig in the aft condition. To rectify this situation we brought an additional five individuals in the labora-

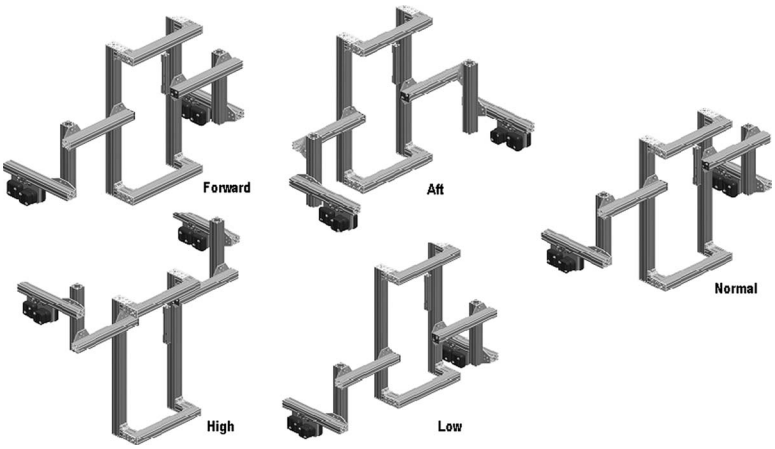

Fig. 4 PLSS rig load configurations (forward, aft, high, low, and normal). The configurations were based on potential design applications for a new PLSS device. The arms of PLSS were designed to sit 15–25 cm from the body in order to allow free motion of the individual's limbs.

tory to test what speed the participants could complete all conditions. Participants, on average, needed a pace of 0.27 m/s (0.6 mph) slower to complete all conditions. Therefore, for the data collection participants selected their pace while walking at 3/8 gravity without the PLSS rig on. Then, the self-selected speed was reduced by 0.27 m/s for all experimental conditions.

Upon arrival at the laboratory on the second day, demographic information (e.g., height, bodyweight (BW), and age) was recorded. Laboratory tennis shoes were provided for the participant to wear, and retroreflective markers were attached using double-sided tape to the metatarsal phalange joint, heel, lateral malleolus, lateral epicondyle, greater trochanter, and acromion-clavicle joint of the right side of the body with double sided tape (Fig. 3).

The BWSS was set to offload the participants by 5/8 of their bodyweight, leaving just 3/8 or Martian bodyweight for them to carry. The participants warmed up by walking in the suspension system without the PLSS rig on. Then, the five load placement conditions (e.g., normal, low, high, forward, and aft) were presented in random order. The appropriate configuration of the PLSS rig was set between conditions. The addition of the PLSS rig adds 20 kg to participants, and this amount was accounted for when offloading the participants with the BWSS. For each condition, participants walked at their self-selected pace for 4 min. In the final three minutes of walking, the positions of the retroreflective markers were recorded with a high speed motion capture system (100 Hz; Vicon Peak, Centennial, CO). The initial minute of unrecorded data was used to allow the participants to reach steady state locomotion prior to data collection. Following each condition, a rest break of at least 3 min was given. Although the activity was not overly strenuous, the rest break insured none of the participants experienced fatigue during data collection.

The positions of the retroreflective markers were digitized using PEAK MOTUS software (Peak Motus, Centennial, CO) and were used to calculate ankle, knee, and hip sagittal plane joint angles. We chose to evaluate the sagittal plane joint dynamics because they represent the dominant plane of motion during walking [30].

We used a technique from Ref. [31] to verify that our data were stationary prior to performing the dynamic stability analyses. Stationarity was evaluated by calculating the mean and standard deviations for 18 randomly selected strides in the ankle, knee, and hip joint patterns for each subject and condition. The means and standard deviations were then plotted, and the slope of this line was calculated. The slopes for each joint were combined and a one sample *t*-test was used to confirm that the slope of the lines were not different from zero. We found the slopes of our means and standard deviations to be no different than zero. This indicated that the mean and variance in the signals were constant over time.

2.4 Floquet Analysis. The kinematics were smoothed with a Butterworth ninth order digital filter with a 6 Hz cut-off. A first central difference method was used to differentiate the filtered angular kinematics. The joint angles and velocities from the continuous time series were extracted for midstance and midswing phase of the gait cycle. These discrete points (i.e., midstance and midswing) were used to construct the Poincaré maps (i.e., plot of a step $(X(n))$ to a subsequent step $(X(n)+1)$) that were used to determine the dynamic stability and joint kinematics used at midstance and midswing (Fig. 5). The instance of midstance was determined to be when the hip angle was positioned at neutral during load bearing. The instance of midswing was determined as maximum knee flexion in the gait cycle. Previous work has shown that eigenvalues calculated at one instance in the stance phase can represent the entire stance phase [32]. Based on this information, we assumed the same is true for the swing phase. The equilibrium value of the Poincaré map of the joint angular positions at midstance and midswing were computed and expressed as means $\pm$ standard deviation. These values were used to determine if the lower extremity joint kinematics changed for the various PLSS load placement conditions. The stability of the gait pattern was partitioned into the swing and stance phases because past biomechanical studies have indicated that the performance of the locomotive system during these phases may represent different balance control mechanisms [11,20,33].

We assumed that the state variables that captured the sagittal plane dynamics of the locomotive system were the joint positions and velocities of the right ankle, knee, and hip at the selected discrete points. These variables were used to define the state vector of the dynamics of the system (Eq. (1))

$$x = [\phi_1, \phi_2, \phi_3, \dot{\phi}_1, \dot{\phi}_2, \dot{\phi}_3]^T \tag{1}$$

The six state variables denote the angular positions (ϕ_1, ϕ_2, ϕ_3) and angular velocities $(\dot{\phi}_1, \dot{\phi}_2, \dot{\phi}_3)$ at the ankle, knee, and hip, respectively. For steady-state human locomotion, the locomotive system achieves dynamic equilibrium. This property is defined by Eq. (2)

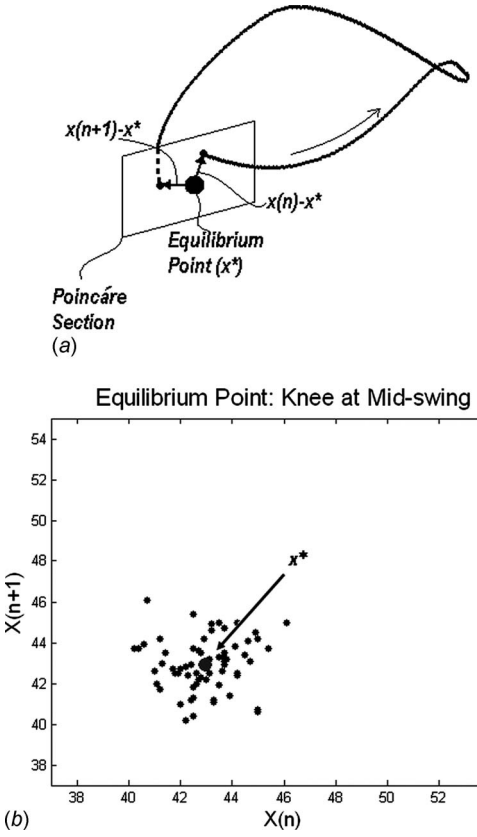

Fig. 5 (*a*) **sample Poincare section in state space transecting the trajectory of the joint pattern. The eigenvalues in FA quantify if the distances between the equilibrium point and each individual step position (e.g., $x(n)$ and $x(n+1)$ grow or decay. (*b*) sample Poincaré map (i.e., plot of a step ($X(n)$) to a subsequent step ($X(n)+1$) of the knee at midswing. The equilibrium point (x^*) for the sample Poincaré map shows that the average knee angular position at midswing was 42.9 deg.**

$$x^* = f(x^*) \tag{2}$$

The variable x^* is the equilibrium point in the Poincaré map, and f is the function that describes the change in the location of the equilibrium point from one step to the next. If the gait pattern was completely periodic (i.e., no deviations in the preferred joint kinematic trajectory), the function would map to the same point on the diagonal of the Poincaré map for every step. However, this is not the case because the locomotion dynamics slightly fluctuates from step to step due to neural errors or disturbances in the coupling of the lower extremity segments. The equilibrium point was estimated by computing the average of all the discrete points in the respective Poincaré maps (Fig. 5).

Perturbations were linearized about the equilibrium point x^* according to Eq. (3)

$$\delta x^{n+1} = J \delta x^n \tag{3}$$

δ denotes the deviation from the equilibrium point, and J is the Jacobian, which defines the rate of change of the state variables from one step to the next. δx^n and δx^{n+1} were defined according to Eqs. (4) and (5), respectively

$$\delta x^n = [x^n - x^*, x^{n+1} - x^*, x^{n+2} - x^*, x^{n+3} - x^*, \ldots] \tag{4}$$

$$\delta x^n = [x^{n+1} - x^*, x^{n+2} - x^*, x^{n+3} - x^*, x^{n+4} - x^*, \ldots] \tag{5}$$

A least-squares algorithm was used to solve for J (Eq. (6)), and the stability of the locomotive pattern was determined by calculating the eigenvalues of J

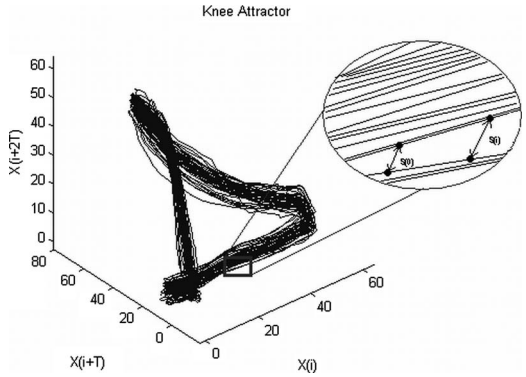

Fig. 6 An example of a knee attractor during locomotion. The euclidian distance between two neighboring points is calculated at two points in time (e.g., $S(0)$ and $S(i)$) to determine the divergence in the system.

$$J = [(\delta x^{n+1})(\delta x^n)^T][(\delta x^n)(\delta x^n)^T]^{-1} \tag{6}$$

The maximum eigenvalue (β) of the system was used to quantify the stability of the swing and stance phase dynamics. A β value that was further away from zero was considered less stable than those that were closer to zero [18,21,32,34]. Theoretically, a locomotive pattern that has a β value closer to one requires a longer time to return back to the steady-state gait pattern than those values near zero.

2.5 Lyapunov Exponent. The ankle, knee, and hip sagittal plane joint angle time series were analyzed unfiltered in order to obtain a more accurate representation of the changes in the local dynamic stability along the attractor flow [35,36]. Standard nonlinear time series analysis techniques were used to quantify the rate of local divergence in the locomotive attractor dynamics (Fig. 6) [37,38]. All calculations were performed using subroutines from TISEAN [39].

The attractor dynamics were reconstructed based on Taken's embedding theorem, which involves using time-lagged copies of the original joint angle time series [37,38]. These time lag copies were used to create a state vector that describes the time evolving dynamics of the locomotive attractor (Eq. (7))

$$y(t) = [x(t), x(t+T), x(t+2T), \ldots x(t+(d_E-1))T] \tag{7}$$

where $y(t)$ is the reconstructed state vector, $x(t)$ is the original time series data, and $x(t+iT)$ is time delay copies of $x(t)$, and d_E is the minimum dimension of the attractor. An average mutual information algorithm was used to determine the appropriate time lag for creating the state vector, and a global false nearest neighbors algorithm was used to determine the attractor dimension [37,38]. The selected time lag was the first local minimum of the average mutual information curve (Fig. 7), and the embedding dimension was identified when the percent false nearest neighbors was nearly zero (Fig. 7).

An algorithm by Rosentein et al. [24] was used to calculate the average LyE for finite changes in the flow of the attractor dynamics (Eq. (8))

$$\lambda(i) = \frac{1}{i}\left(\frac{1}{M}\sum_{j=1}^{M-i} \ln\frac{s_j(i)}{s_j(0)}\right) \tag{8}$$

where λ is the LyE, i is the data sample, M is the number of points in the attractor that are considered, $s_j(0)$ is the initial Euclidean distance between the j neighbors, and $s_j(i)$ is the Euclidean distance between the j neighbors i times later. The finite divergences of the attractor flow were used to construct a divergence curve consisting of the average rate of divergence of neighboring points in the attractor as a function of time (Fig. 8). The abscissa of the

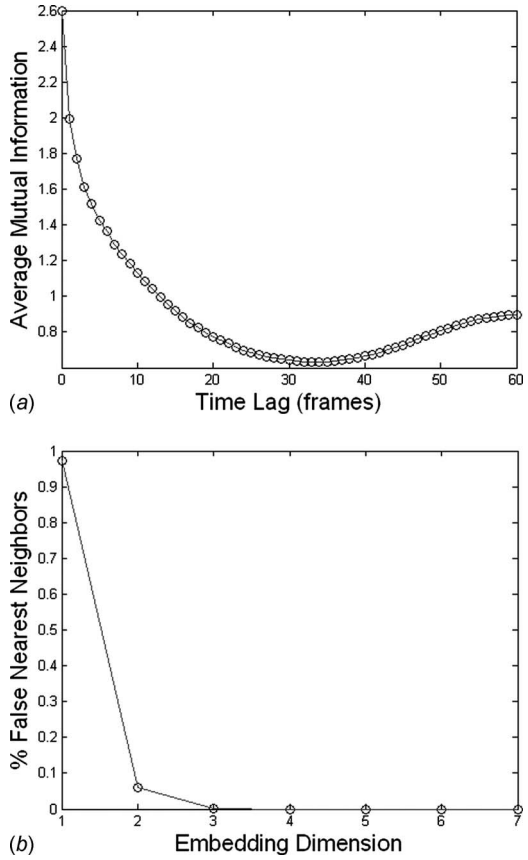

Fig. 7 (*a*) **the time lag is determined to be at the first local minimum of the curve, which in this case is at 34 frames.** (*b*) **the embedding dimension is determined when the global false nearest neighbors curves drop to zero, indicating no false neighbors are present in the data. Here the embedding dimension would be 4.**

divergence curve was rescaled by multiplying it by the average stride frequency in order to normalize the curve to the individual's gait cycle frequency. The average largest LyE was estimated by using a least-squares algorithm to calculate the slope of the linear region of the first two strides of the divergence curve (Fig. 8). A larger slope indicates there is a greater rate of local divergence in the attractor [24].

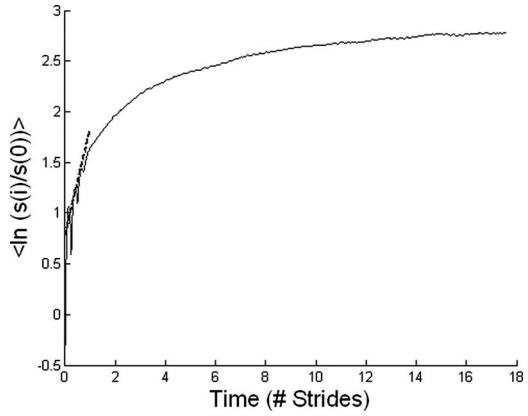

Fig. 8 The linear region of the divergence curve was used to calculate the slope. The slope of the curve indicates the average rate of local divergence in the reconstructed attractor.

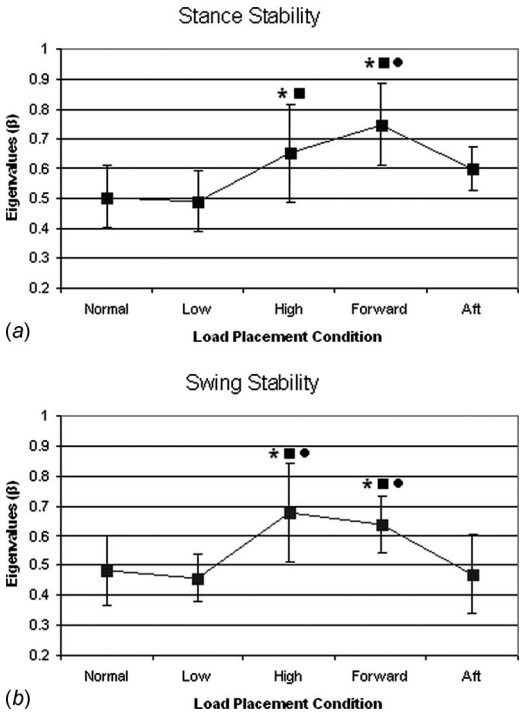

Fig. 9 β **values for stance and swing during the different load locations.** $*$ **denotes significantly different from normal,** ■ **denotes significantly different from low, and** ● **denotes significantly different from aft.**

Maximum LyE were calculated for the ankle, knee, and hip joint separately. The results for each individual joint were similar; therefore, we pooled the data from all three joints to give an overall representation of the dynamic stability of the locomotive pattern.

2.6 Statistical Analysis. One-way repeated measures ANOVAs were used to determine differences in load location with Tukey HSD for post-hoc analysis. Alpha was set to 0.05.

3 Results

3.1 Floquet Analysis. The PLSS load placement did have a significant influence on the dynamic stability of the gait pattern during stance ($F(4,36)=7.08$, $p=0.0001$; Fig. 9) and swing ($F(4,36)=7.37$, $p=0.0001$; Fig. 9). During stance, the normal and low load placements were significantly more stable than the high ($p=0.04$ and $p=0.002$, respectively) and forward ($p=0.01$ and $p=0.001$, respectively) load locations. Aft load placement was also significantly more dynamically stable than the forward load placement ($p=0.02$). During the swing phase, the normal, low, and aft load placement conditions remained significantly more dynamically stable than the forward load placement ($p=0.03$, $p=0.001$, and $p=0.01$, respectively), and also demonstrated greater dynamic stability than the high load placement ($p=0.01$, $p=0.002$, and $p=0.01$, respectively). In overall consideration of the gait cycle, the results indicate the gait pattern is more dynamically stable with loads in the normal condition and low condition. The forward and high load placement appears to be more unstable than most conditions. The aft load placement was significantly more dynamically stable than the high and forward load placements during swing, but was only more stable than the forward condition during stance.

No differences were found in the angular displacement of the ankle joint during stance ($F(4,36)=0.70$, $p=0.60$) and swing ($F(4,36)=0.87$, $p=0.49$; Figs. 10 and 11). However, high vari-

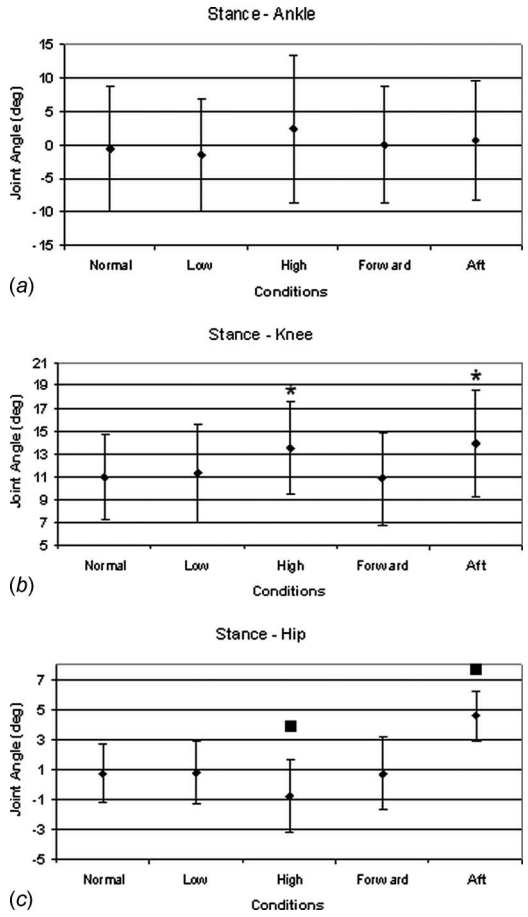

Fig. 10 The equilibrium points (i.e., average joint positions ±SD) during midstance for the ankle, knee, and hip in each load placement condition. ∗ denotes significantly different from normal, low, and forward, while ■ denotes significantly different from all other conditions.

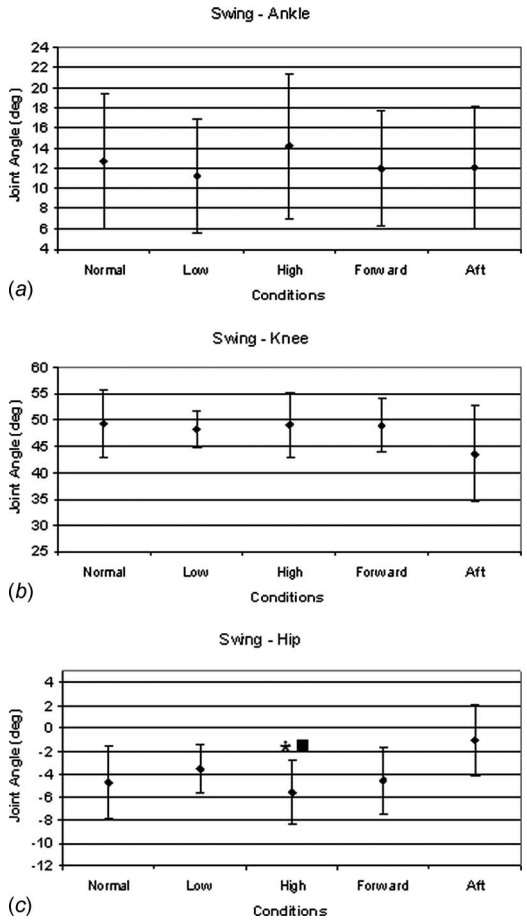

Fig. 11 The equilibrium points (i.e., average joint positions ±SD) during midswing for the ankle, knee and hip in each load placement condition. ∗ denotes significantly different from low and ■ denotes significant different from aft.

ability in the ankle joint positions during stance should be noted. Inspection of individual participants reveals a difference in strategy while walking in the load placement conditions. Some participants have their ankle plantar flexed at midstance indicating a forefoot walking strategy. The number of participants using this strategy changed depending on the condition (Fig. 12). At the knee, during stance, different joint positions were found ($F(4,36)=5.72$, $p=0.001$); however, during the swing phase no differences were found ($F(4,36)=2.36$, $p=0.07$; Figs. 10 and 11). During stance, the knee had greater flexion during the high and aft load positions than the normal, low, and forward positions. Results indicated that hip joint strategies changed between conditions during the stance ($F(4,36)=13.46$, $p=0.0001$) and swing phases ($F(4,36)=4.78$, $p=0.003$; Figs. 10 and 11). During stance, the hip required greater flexion during the aft placement than all other conditions. Additionally, during the high load position participants exhibited hip extension at midstance; while all other conditions included a slightly flexed position. During the swing phase, the high load placement required greater hip extension than the low and aft load placements.

3.2 Lyapunov Exponent. The time lag and embedding dimension used to calculate maximum LyE were 31 and 5, respectively. These values were based on compiling the results for all subjects and joints, which resulted in the means and standard deviations of 31 ± 5 and 5 ± 0.5, respectively. Unlike FA, no significant differences were found in dynamic stability between conditions using maximum LyE ($F(4,36)=1.67$, $p=0.17$; Fig. 13). These results indicated that varying the position of load does not appear to influence the average local instabilities present in the gait pattern.

4 Discussion

Our hypothesis that load placement can impact the dynamic stability of the locomotive pattern was supported by the Floquet analysis results. During the stance and swing phases of walking, loads that were placed ahead of the torso (i.e., forward condition) and high on the torso (i.e., high condition) generated significantly less dynamically stable walking patterns than walking with load at the sides of the torso (i.e., normal condition) and low on the body

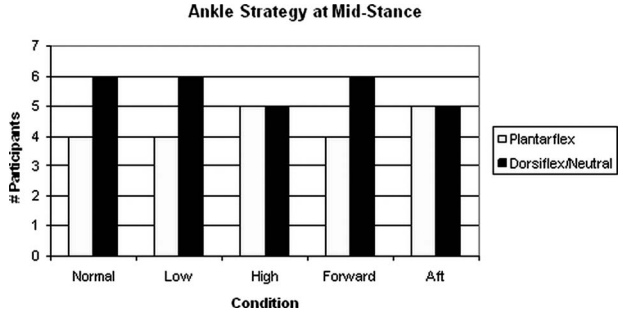

Fig. 12 The number of participants that walked with the ankle dorsiflexed (forefoot strike) and plantarflexed at midstance

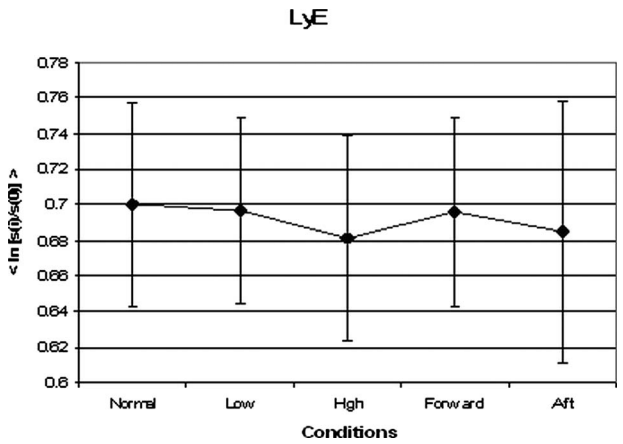

Fig. 13 Maximum LyE values for the five load placement conditions. No significant differences were found between conditions ($p > 0.05$).

(i.e., low condition). In both the stance and swing phases, the forward and high condition caused a decrease in the dynamic stability of the gait pattern. Walking has been described as a controlled fall, where each successive step is responsible for catching the body as it falls forward [40]. Forward load placement could be detrimental to the dynamic stability of the walking pattern because it may increase the forward and downward momentum of the body between steps, which could make the step-to-step transition more difficult. Furthermore, loads that were placed high on the PLSS rig were the furthest from the individual's natural center of gravity, and may have caused greater torque to be generated if the body were to shift slightly forward or backward.

Mixed results were noted for carrying loads behind the torso (i.e., aft condition) where it was more dynamically stable than the forward condition, but not the high condition during stance. However, during swing, the aft condition was more stable than both forward and high. The mixed results may be related to the changes in the lower extremity kinematics that occurred while carrying loads behind the torso. Additionally, the high condition appeared to cause some kinematic changes that many of the other conditions did not. During the stance phase, the high and aft load placements required participants to walk with greater knee flexion at midstance. Additionally, the high load placement required hip extension, while all other conditions required hip flexion at midstance. Hip extension may have been necessary for the participants to keep the load over their base of support. Thus, the participants may have been working to keep the high load directly above their torso to avoid excessive torque. The aft condition had greater hip flexion than the normal, low, and forward load placements. In the aft load placement, participants were forced to drive their legs forward to generate additional momentum for when the heel touches down and weight is transferred to the leading foot [40]. During the swing phase, the high load placement required greater hip extension than the low condition (i.e., participants were still trying to keep the load directly above their base of support), while the aft load placement required less hip extension (i.e., participants were still driving the leg by putting the hip in a more flexed position). Potentially, these kinematic adjustments are indicators of the challenge the high and aft load placements applied to the locomotive system. The kinematic findings may also indicate the knee and hip are important joints for maintaining dynamic stability in simulated Martian gravity while carrying loads in different positions.

Even though, the joint positions were not significantly different at the ankle, in most conditions nearly half the participants were on their forefoot at midstance, while the other half utilized a more typical heel-to-toe walking pattern. In the high and aft conditions, an additional study participant had a forefoot posture at midstance, which may be a further indicator of the difficulty of these two walking conditions. Previously it has been shown, the ankle is an important factor for generating locomotion in reduced gravity while the hip and knee remained unaltered [41]. Our results indicated that the differences in the ankle kinematics may be related to individual strategies for maintaining the dynamic stability of the locomotive pattern. Since the experiment by Thelkeld et al. [41] did not include load carrying, it is to be expected that their findings at the knee and hip differ from ours. Some load carrying studies have shown changes in the knee and hip joint to accommodate for load [2,20], while other studies have shown no kinematic adaptations at all [42,43]. These studies evaluated load carrying in Earth's gravity; whereas, our experiment changed the positions of load in simulated Martian gravity, which may explain why our results differ. In this study, all joints appear to be important for the dynamic stability of the sagittal plane locomotive pattern, when the load placement is altered and gravity is reduced.

Our findings support the early comments of Parkes [8], where he suggested that loads placed near the torso and low would be best for stable and comfortable walking. Additionally, the findings by Kinoshita [2] demonstrated some potential stabilizing mechanisms in the walking pattern while carrying loads on the back and in a double pack, which placed load on the back and chest. Alternatively, Arellano et al. [20], who evaluated dynamic stability directly, found no changes in stability while walking with added load. Potentially, the findings by Arellano et al. [20] were due to the evenly distributed load about the waist (i.e., keeping the load low and evenly distributed); whereas, the Kinoshita [2] study had load placed only on the back or in a pack that placed load in front and behind the upper torso. Furthermore, participants in the Legg and Mahanty [4] study reported a perceived improved stability when the load was distributed evenly about the torso in a weighted vest or load distributed in packs placed on the front and back of the torso. In an analysis of postural stability limits, it was determined that external load positions, which lowered the location of the center of gravity extended stability limits [44]. Altogether these results support our findings that evenly distributed loads generate more dynamically stable walking patterns.

Our hypothesis that the local dynamic stability of the gait pattern was influenced by load placement of the PLSS rig was not supported. Previous experimental work with humans and simulations from computer walking models have suggested that the Lyapunov measure of the local instabilities present in the gait pattern is more sensitive to changes in walking stability than Floquet analysis [45,46]. However, the results presented here do not appear to support this notion. We suggest that the local instabilities present in the flow of the attractor dynamics may have to grow sufficiently large before a loss of dynamic stability will occur. Alternatively, our perceived lack of significant changes in the local dynamic stability may be related to the numerical method we used for estimating maximum Lyapunov exponent [47]. The Rosenstein et al. algorithm is based on an arithmetic average that assumes that the local instabilities across the attractor dynamics are relatively constant (Eq. (2)). However, this is not true in many dynamical systems (e.g., Lorenz and Rossler system) that have local instabilities in certain parts of the attractor and local stability present in other parts of the attractor dynamics [47]. Hence, the short time scale instabilities may have been overlooked because they were averaged with the regions of the attractor that were convergent [23,47]. Based on this notion, it is possible that there may have been short-time local instabilities in certain portions of the gait cycle that were not detected with the Lyapunov exponent numerical methods used in this investigation. We suggest that future investigations of dynamic stability should consider evaluating the evolution of the local instabilities in the gait dynamics over smaller regions of specific portions of the gait cycle (i.e., stance and swing). On the other hand, our difficulties in finding significant changes in the largest LyE values may be related to our

selection of the scaling region of the divergence curve (Fig. 2). Our rationale for measuring the slope of the initial portion of the divergence curve was based on the methodology presented in previous human gait experiments [45,48–51]. However, for the Rosenstien algorithm to work properly one needs to have a clear linear scaling region of the divergence curve. It is possible that our LyE values were inconclusive because they were estimated from the initial region of the divergence curve, where it is noise dominated. Possibly, better estimates of the LyE could be achieved with the Rosenstein algorithm by using more points to improve resolution or by increasing sampling frequency. However, we suggest this would most likely not influence our results because the number of data samples used in this investigation and sampling frequency was well beyond what has been previously reported for stable estimates of the largest LyE for human walking with the Rosenstein algorithm [45,48–51]. Further exploration of the technical issues associated with selecting a scaling region of the divergence curve to estimate the amount of divergence in physiological rhythms with the Rosenstein algorithm is warranted before strong conclusions can be made about the effects of the local divergences on the overall stability of the walking pattern.

Stretching of the surgical tubing to a proper length was important for achieving a linear response from the BWSS used in this experiment. In most cases, the surgical tubing was stretched from two to three times its original length. We assumed that the stretch placed on the tubing was enough to place it within a small linear region of the nonlinear stress-strain curve of the elastic material. Furthermore, we assumed that the vertical fluctuations of the center of mass were small enough such that they were bounded to remain within this linear region. Our load cell data indicated the restoring forces supplied by the BWSS was within $\pm 7\%$ of the offloading goal. Additionally, the BWSS may supply some stabilizing forces. Our system was built on a low friction trolley that allowed movement in the anterior-posterior direction. Although we took care in its design, it is possible that there may have been some friction in the trolley that could have influenced our results. More importantly, it is possible that the BWSS may have provided additional stabilizing forces in the frontal plane. We elected to allow the system to provide greater stabilizing forces in this plane because review of the Apollo mission video displayed a large number of falls that occurred in the sagittal plane (e.g., the astronauts were toppling forward). Last, although some stabilizing forces may be introduced by the BWSS, these forces were present for all load placement conditions allowing us to compare across conditions.

The preferred mode of locomotion in reduced gravity is unclear. The Apollo mission archives revealed several astronauts elected to hop or lope while moving across the lunar terrain. It is unknown if this selection of locomotion was due to reduced gravity or the space suit design. The Apollo suit design restricted the motion of the hip, knee and ankle. Walking and running would be difficult without the ability to freely move these joints. In a recent unpublished experiment aboard NASA's C-9 parabolic flight aircraft, participants in a descriptive study of locomotion in lunar and Martian gravity were asked to try all modes of locomotion including hopping and loping. Participants preferred walking or running to the loping style of locomotion. This may indicate that the suit was the reason for the loping we saw in the Apollo missions. With this recent experiment in mind, and noting that the participants in the current study were allowed to use any form of locomotion they preferred, we believe our findings of a walking gait style to be reasonable.

5 Conclusion

Based on the Floquet analysis results, PLSS loads at the side of the torso and low on the body improve dynamic stability of the gait pattern in simulated Martian gravity. Furthermore, loads placed in the normal and low positions did not require modifications to the lower extremity kinematics to the extent that the high and aft load positions did. Our results infer that space scientists and engineers should consider developing a PLSS that evenly distributes the load and maintains the load low on the torso. Additionally, in the development of the next generation space suit, engineers may consider the importance of the sagittal plane mobility of all three lower extremity joints since our kinematic results indicate that they were influenced by the load placement of the PLSS rig. Previous suit designs have not provided free motion of the hip, knee, and ankle [52]. We suggest that maintaining the dynamic stability of the walking pattern may become more difficult if the sagittal plane degrees of freedom are constrained by the space suit.

Acknowledgment

We would like to thank Kristin Reddoch and Fatima Garcia for their assistance in collecting this data. In addition, we want to thank Dr. Rodger Kram for his insight on the design of our BWSS, and the NASA EPSP group for supplying the PLSS rig used in the investigation. This work was funded by NASA Grant No. NNX07AP91A and the Texas Space Grant Consortium.

References

[1] Datta, S. R., and Ramanathan, N. L., 1971, "Ergonomic Comparison of Seven Modes of Carrying Loads on the Horizontal Plane," Ergonomics, **14**(2), pp. 269–278.
[2] Kinoshita, H., 1985, "Effects of Different Loads and Carrying Systems on Selected Biomechanical Parameters Describing Walking Gait," Ergonomics, **28**(9), pp. 1347–1362.
[3] Knapik, J. J., Ang, P., Meiselman, H., Johnson, W., Kirk, J., Bensel, C., and Hanlon, W., 1997, "Soldier Performance and Strenuous Road Marching: Influence of Load Mass and Load Distribution," Mil. Med., **162**(1), pp. 62–67.
[4] Legg, S. J., and Mahanty, A., 1985, "Comparison of Five Modes of Carrying a Load Close to the Trunk," Ergonomics, **28**(12), pp. 1653–1660.
[5] Lloyd, R., and Cooke, C. B., 2000, "The Oxygen Consumption Associated With Unloaded Walking and Load Carriage Using Two Different Backpack Designs," Eur. J. Appl. Physiol., **81**(6), pp. 486–492.
[6] Courtemanche, R., Teasdale, N., Boucher, P., Fleury, M., Lajoie, Y., and Bard, C., 1996, "Gait Problems in Diabetic Neuropathic Patients," Arch. Phys. Med. Rehabil., **77**(9), pp. 849–855.
[7] Dingwell, J. B., Cusumano, J. P., Sternad, D., and Cavanagh, P. R., 2000, "Slower Speeds in Patients With Diabetic Neuropathy Lead to Improved Local Dynamic Stability of Continuous Overground Walking," J. Biomech., **33**(10), pp. 1269–1277.
[8] Parkes, E. A., 1869, *A Manual of Practical Hygiene: Prepared Especially for Use in the Medical Service of the Army*, Churchill, London.
[9] Carr, C. E., 2005, "The Bioenergetics of Walking and Running in Space Suits," Ph.D. dissertation, Massachusetts Institute of Technology, Cambridge, MA.
[10] Bauby, C. E., and Kuo, A. D., 2000, "Active Control of Lateral Balance in Human Walking," J. Biomech., **33**(11), pp. 1433–1440.
[11] Gabell, A., and Nayak, U. S., 1984, "The Effect of Age on Variability in Gait," J. Gerontol., **39**(6), pp. 662–666.
[12] Owings, T. M., and Grabiner, M. D., 2004, "Variability of Step Kinematics in Young and Older Adults," Gait and Posture, **20**(1), pp. 26–29.
[13] Owings, T. M., and Grabiner, M. D., 2004, "Step Width Variability, But Not Step Length Variability or Step Time Variability, Discriminates Gait of Healthy Young and Older Adults During Treadmill Locomotion," J. Biomech., **37**(6), pp. 935–938.
[14] Cordero, A. F., Koopman, H. J., and van der Helm, F. C., 2004, "Mechanical Model of the Recovery From Stumbling," Biol. Cybern., **91**(4), pp. 212–220.
[15] Pavol, M. J., Owings, T. M., Foley, K. T., and Grabiner, M. D., 1999, "Gait Characteristics as Risk Factors for Falling From Trips Induced in Older Adults," J. Gerontol., Ser. A, **54**(11), pp. 583–590.
[16] Pavol, M. J., Owings, T. M., Foley, K. T., and Grabiner, M. D., 1999, "The Sex and Age of Older Adults Influence the Outcome of Induced Trips," J. Gerontol., Ser. A, **54**(2), pp. M103–108.
[17] Schillings, A. M., van Wezel, B. M., and Duysens, J., 1996, "Mechanically Induced Stumbling During Human Treadmill Walking," J. Neurosci. Methods, **67**(1), pp. 11–17.
[18] Full, R., Kubow, T., Schmitt, J., Holmes, P., and Koditschek, D., 2002, "Quantifiying Dynamic Stability and Maneuverability in Legged Locomotion," Integr. Comp. Biol., **42**, pp. 149–157.
[19] Holmes, P., Full, R., Koditschek, D., and Guckenheimer, J., 2006, "The Dynamics of Legged Locomotion: Models, Analyses, and Challenges," SIAM Rev., **48**(2), pp. 207–304.
[20] Arellano, C. J., Layne, C. S., O'Connor, D. P., Scott-Pandorf, M. M., and Kurz, M. J., 2009, "Does Load Carrying Influence Sagittal Plane Locomotive Stability?" Med. Sci. Sports Exercise, **41**(3), pp. 620–627.
[21] McGeer, T., 1990, "Passive Dynamic Walking," Int. J. Robot. Res., **9**(2), pp. 62–82.
[22] Granata, K. P., and Lockhart, T. E., 2008, "Dynamic Stability Differences in

Fall-Prone and Healthy Adults," J. Electromyogr Kinesiol, **18**, pp. 172–178.
[23] Ali, F., and Menzinger, M., 1999, "On the Local Stability of Limit Cycles," Chaos, **9**(2), pp. 348–356.
[24] Rosenstein, M. T., Collins, J. J., and De Luca, C. J., 1993, "A Practical Method for Calculating Largest Lyapunov Exponents From Small Data Sets," Physica D, **65**, pp. 117–134.
[25] Baker, G. L., Gollub, J. P., and Blackburn, J. A., 1996, "Inverting Chaos: Extracting System Parameters From Experimental Data," Chaos, **6**(4), pp. 528–533.
[26] Buzzi, U. H., Stergiou, N., Kurz, M. J., Hageman, P. A., and Heidel, J., 2003, "Nonlinear Dynamics Indicates Aging Affects Variability During Gait," Clin. Biomech. (Bristol, Avon), **18**(5), pp. 435–443.
[27] Dingwell, J. B., and Cusumano, J., 2000, "Nonlinear Time Series Analysis of Normal and Pathological Human Walking," Chaos, **10**(4), pp. 848–863.
[28] Kurz, M. J., and Stergiou, N., 2005, "An Artificial Neural Network That Utilizes Hip Joint Actuations to Control Bifurcations and Chaos in a Passive Dynamic Bipedal Walking Model," Biol. Cybern., **93**(3), pp. 213–221.
[29] Thomas, S., Reading, J., and Shephard, R. J., 1992, "Revision of the Physical Activity Readiness Questionnaire (PAR-Q)," Can. J. Sport Sci., **17**(4), pp. 338–345.
[30] Mah, C. D., Hulliger, M., Lee, R. G., and O'Callaghan, I. S., 1994, "Quantitative Analysis of Human Movement Synergies: Constructive Pattern Analysis for Gait," J. Motor Behav., **26**(2), pp. 83–102.
[31] Chau, T., Chau, D., Casas, M., Berall, G., and Kenny, D. J., 2005, "Investigating the Stationarity of Paediatric Aspiration Signals," IEEE Trans. Neural Syst. Rehabil. Eng., **13**(1), pp. 99–105.
[32] Hurmuzlu, Y., and Basdogan, C., 1994, "On the Measurement of Dynamic Stability of Human Locomotion," ASME J. Biomech. Eng., **116**(1), pp. 30–36.
[33] Frenkel-Toledo, S., Giladi, N., Peretz, C., Herman, T., Gruendlinger, L., and Hausdorff, J. M., 2005, "Effect of Gait Speed on Gait Rhythmicity in Parkinson's Disease: Variability of Stride Time and Swing Time Respond Differently," J. Neuroeng. Rehabil., **2**, pp. 23–29.
[34] Hurmuzlu, Y., Basdogan, C., and Stoianovici, D., 1996, "Kinematics and Dynamic Stability of the Locomotion of Post-Polio Patients," ASME J. Biomech. Eng., **118**(3), pp. 405–411.
[35] Rapp, P. E., 1994, "A Guide to Dynamical Analysis," Integr Physiol. Behav. Sci., **29**(3), pp. 311–327.
[36] Stergiou, N., Buzzi, U. H., Kurz, M. J., and Heidel, J., 2004, "Nonlinear Tools in Human Movement," *Innovative Analysis of Human Movement*, N. Stergiou, ed., Human Kinetics, Champaign, IL.
[37] Abarbanel, H. D. I., 1996, *Analysis of Observed Chaotic Data*, Springer, New York.
[38] Kantz, H., and Schreiber, T., 2004, *Nonlinear Time Series Analysis*, Cambridge University Press, Cambridge, UK.
[39] Hegger, R., Kantz, H., and Schreiber, T., 1999, "Practical Implication of Nonlinear Time Series Methods: The Tisean Package," Chaos, **9**(2), pp. 413–435.
[40] Hsiang, S. M., and Chang, C., 2002, "The Effect of Gait Speed and Load Carrying on the Reliability of Ground Reaction Forces," Safety Sci., **40**, pp. 639–657.
[41] Threlkeld, A. J., Cooper, L. D., Monger, B. P., Craven, A. N., and Haupt, H. G., 2003, "Temporospatial and Kinematic Gait Alterations During Treadmill Walking With Body Weight Suspension," Gait and Posture, **17**(3), pp. 235–245.
[42] Browning, R. C., Modica, J. R., Kram, R., and Goswami, A., 2007, "The Effects of Adding Mass to the Legs on the Energetics and Biomechanics of Walking," Med. Sci. Sports Exercise, **39**(3), pp. 515–525.
[43] Holt, K. G., Wagenaar, R. C., LaFiandra, M. E., Kubo, M., and Obusek, J. P., 2003, "Increased Musculoskeletal Stiffness During Load Carriage at Increasing Walking Speeds Maintains Constant Vertical Excursion of the Body Center of Mass," J. Biomech., **36**(4), pp. 465–471.
[44] Holbein, M. A., and Redfern, M. S., 1997, "Functional Stability Limits While Holding Loads in Various Positions," Int. J. Ind. Ergonom., **19**, pp. 387–395.
[45] Dingwell, J. B., and Kang, H. G., 2007, "Differences Between Local and Orbital Dynamic Stability During Human Walking," ASME J. Biomech. Eng., **129**(4), pp. 586–593.
[46] Su, J. L., and Dingwell, J. B., 2007, "Dynamic Stability of Passive Dynamic Walking on an Irregular Surface," ASME J. Biomech. Eng., **129**(6), pp. 802–810.
[47] Smith, L. A., Ziehmann, C., and Fraedrich, K., 1999, "Uncertainty Dynamics and Predictability in Chaotic Systems," Q. J. R. Meteorol. Soc., **125**, pp. 2855–2886.
[48] Dingwell, J. B., and Cavanagh, P., 2001, "Increased Variability of Continuous Overground Walking in Neuropathic Patients is Only Indirectly Related to Sensory Loss," Gait and Posture, **14**(1), pp. 1–10.
[49] Dingwell, J. B., and Marin, L. C., 2006, "Kinematic Variability and Local Dynamic Stability of Upper Body Motions When Walking at Different Speeds," J. Biomech., **39**(3), pp. 444–452.
[50] England, S. A., and Granata, K. P., 2007, "The Influence of Gait Speed on Local Dynamic Stability of Walking," Gait and Posture, **25**(2), pp. 172–178.
[51] Kang, H. G., and Dingwell, J. B., 2006, "Intra-Session Reliability of Local Dynamic Stability of Walking," Gait and Posture, **24**(3), pp. 386–390.
[52] Newman, D. J., and Barrat, M., 1997, "Life Support and Performance Issues for Extravehicular Activity (EVA)," *Fundamentals of Space Life Sciences*, S. Churchill, ed., Krieger, Melbourne, FL.